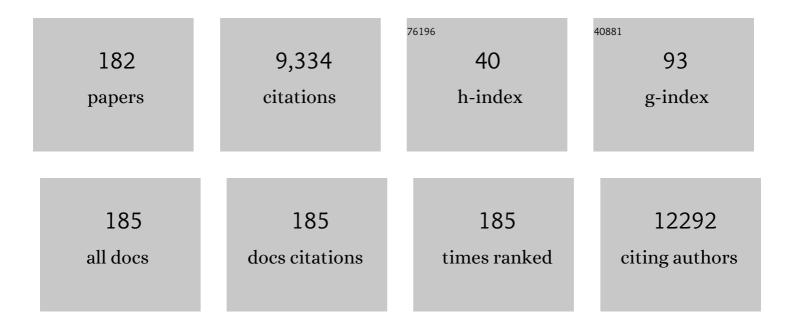
List of Publications by Year in descending order

Source: https://exaly.com/author-pdf/9517710/publications.pdf Version: 2024-02-01



#	Article	IF	CITATIONS
1	Epitaxial growth of a monolayer WSe ₂ -MoS ₂ lateral p-n junction with an atomically sharp interface. Science, 2015, 349, 524-528.	6.0	1,009
2	Large-Area Synthesis of Highly Crystalline WSe ₂ Monolayers and Device Applications. ACS Nano, 2014, 8, 923-930.	7.3	885
3	Plasmonic Nanolaser Using Epitaxially Grown Silver Film. Science, 2012, 337, 450-453.	6.0	686
4	Monolayer MoSe ₂ Grown by Chemical Vapor Deposition for Fast Photodetection. ACS Nano, 2014, 8, 8582-8590.	7.3	515
5	Wafer-scale single-crystal hexagonal boron nitride monolayers on CuÂ(111). Nature, 2020, 579, 219-223.	13.7	409
6	Second Harmonic Generation from Artificially Stacked Transition Metal Dichalcogenide Twisted Bilayers. ACS Nano, 2014, 8, 2951-2958.	7.3	388
7	Bandgap tunability at single-layer molybdenum disulphide grain boundaries. Nature Communications, 2015, 6, 6298.	5.8	358
8	Spectroscopic Signatures for Interlayer Coupling in MoS ₂ –WSe ₂ van der Waals Stacking. ACS Nano, 2014, 8, 9649-9656.	7.3	288
9	Efficient Single-Photon Sources Based on Low-Density Quantum Dots in Photonic-Crystal Nanocavities. Physical Review Letters, 2006, 96, 117401.	2.9	244
10	Roomâ€Temperature Ferroelectricity in Hexagonally Layered αâ€In ₂ Se ₃ Nanoflakes down to the Monolayer Limit. Advanced Functional Materials, 2018, 28, 1803738.	7.8	241
11	Multidirection Piezoelectricity in Mono- and Multilayered Hexagonal α-In ₂ Se ₃ . ACS Nano, 2018, 12, 4976-4983.	7.3	215
12	Purely in-plane ferroelectricity in monolayer SnS at room temperature. Nature Communications, 2020, 11, 2428.	5.8	214
13	All-Color Plasmonic Nanolasers with Ultralow Thresholds: Autotuning Mechanism for Single-Mode Lasing. Nano Letters, 2014, 14, 4381-4388.	4.5	201
14	Photoluminescence Enhancement and Structure Repairing of Monolayer MoSe ₂ by Hydrohalic Acid Treatment. ACS Nano, 2016, 10, 1454-1461.	7.3	179
15	Optically initialized robust valley-polarized holes in monolayer WSe2. Nature Communications, 2015, 6, 8963.	5.8	151
16	Layered MoS ₂ grown on <i>c</i> â€sapphire by pulsed laser deposition. Physica Status Solidi - Rapid Research Letters, 2015, 9, 187-191.	1.2	130
17	Heteroepitaxial growth of wurtzite InN films on Si(111) exhibiting strong near-infrared photoluminescence at room temperature. Applied Physics Letters, 2004, 84, 3765-3767.	1.5	128
18	Bidirectional Allâ€Optical Synapses Based on a 2D Bi ₂ 0 ₂ Se/Graphene Hybrid Structure for Multifunctional Optoelectronics. Advanced Functional Materials. 2020, 30, 2001598.	7.8	123

#	Article	IF	CITATIONS
19	Band Gapâ€Tunable Molybdenum Sulfide Selenide Monolayer Alloy. Small, 2014, 10, 2589-2594.	5.2	109
20	Ledge-directed epitaxy of continuously self-aligned single-crystalline nanoribbons of transition metal dichalcogenides. Nature Materials, 2020, 19, 1300-1306.	13.3	104
21	Evidence of indirect gap in monolayer WSe2. Nature Communications, 2017, 8, 929.	5.8	98
22	Negative circular polarization emissions from WSe2/MoSe2 commensurate heterobilayers. Nature Communications, 2018, 9, 1356.	5.8	88
23	Controllable Synthesis of Band-Gap-Tunable and Monolayer Transition-Metal Dichalcogenide Alloys. Frontiers in Energy Research, 2014, 2, .	1.2	84
24	Moiré potential impedes interlayer exciton diffusion in van der Waals heterostructures. Science Advances, 2020, 6, .	4.7	83
25	Photocurrent studies of the carrier escape process from InAs self-assembled quantum dots. Physical Review B, 2000, 62, 6959-6962.	1.1	81
26	Tuning the energy levels of self-assembled InAs quantum dots by rapid thermal annealing. Applied Physics Letters, 2000, 76, 691-693.	1.5	80
27	Band Alignment of 2D Transition Metal Dichalcogenide Heterojunctions. Advanced Functional Materials, 2017, 27, 1603756.	7.8	74
28	Layer-Dependent and In-Plane Anisotropic Properties of Low-Temperature Synthesized Few-Layer PdSe ₂ Single Crystals. ACS Nano, 2020, 14, 4963-4972.	7.3	64
29	Largeâ€Area 2D Layered MoTe ₂ by Physical Vapor Deposition and Solidâ€Phase Crystallization in a Telluriumâ€Free Atmosphere. Advanced Materials Interfaces, 2017, 4, 1700157.	1.9	61
30	Direct measurement of piezoelectric field in In[sub 0.23]Ga[sub 0.77]N/GaN multiple quantum wells by electrotransmission spectroscopy. Journal of Applied Physics, 2002, 91, 531.	1.1	59
31	Photoluminescence properties of self-assembled InN dots embedded in GaN grown by metal organic vapor phase epitaxy. Applied Physics Letters, 2006, 88, 191913.	1.5	58
32	Room-temperature electroluminescence at 1.3 and 1.5â€,μm from Ge/Si self-assembled quantum dots. Applied Physics Letters, 2003, 83, 2958-2960.	1.5	57
33	Diamagnetic Response of Exciton Complexes in Semiconductor Quantum Dots. Physical Review Letters, 2008, 101, 267402.	2.9	57
34	Tailoring excitonic states of van der Waals bilayers through stacking configuration, band alignment, and valley spin. Science Advances, 2019, 5, eaax7407.	4.7	56
35	Hole emission processes in InAs/GaAs self-assembled quantum dots. Physical Review B, 2002, 66, .	1.1	47
36	Investigations on Diamond Nanostructuring of Different Morphologies by the Reactive-Ion Etching Process and Their Potential Applications. ACS Applied Materials & Interfaces, 2013, 5, 7439-7449.	4.0	46

#	Article	IF	CITATIONS
37	Dielectric impact on exciton binding energy and quasiparticle bandgap in monolayer WS ₂ and WSe ₂ . 2D Materials, 2019, 6, 025028.	2.0	44
38	Synthesis and structure of two-dimensional transition-metal dichalcogenides. MRS Bulletin, 2015, 40, 566-576.	1.7	43
39	Carrier dynamics of type-II InAsâ^•GaAs quantum dots covered by a thin GaAs1â^'xSbx layer. Applied Physics Letters, 2008, 93, .	1.5	41
40	Effects of thermal annealing on the emission properties of type-II InAs/GaAsSb quantum dots. Applied Physics Letters, 2009, 94, 053101.	1.5	40
41	High On-State Current in Chemical Vapor Deposited Monolayer MoS ₂ nFETs With Sn Ohmic Contacts. IEEE Electron Device Letters, 2021, 42, 272-275.	2.2	38
42	Characterization of GaN Schottky barrier photodetectors with a low-temperature GaN cap layer. Journal of Applied Physics, 2003, 94, 1753-1757.	1.1	37
43	Low-defect-density WS2 by hydroxide vapor phase deposition. Nature Communications, 2022, 13, .	5.8	37
44	Metalâ€Guided Selective Growth of 2D Materials: Demonstration of a Bottomâ€Up CMOS Inverter. Advanced Materials, 2019, 31, e1900861.	11.1	36
45	Quantum-confined Stark shift in electroreflectance of InAs/InxGa1â^'xAs self-assembled quantum dots. Applied Physics Letters, 2001, 78, 1760-1762.	1.5	34
46	Large-area few-layer MoS ₂ deposited by sputtering. Materials Research Express, 2016, 3, 065007.	0.8	34
47	Effects of GaAsSb capping layer thickness on the optical properties of InAs quantum dots. Applied Physics Letters, 2011, 99, 073108.	1.5	31
48	Effects of spacer thickness on optical properties of stacked Ge/Si quantum dots grown by chemical vapor deposition. Journal of Applied Physics, 2003, 93, 4999-5002.	1.1	30
49	Impacts of structural asymmetry on the magnetic response of excitons and biexcitons in single self-assembled In(Ga)As quantum rings. Physical Review B, 2009, 80, .	1.1	29
50	Self-assembled free-standing colloidal crystals. Nanotechnology, 2005, 16, 1440-1444.	1.3	28
51	Anticorrelation between the splitting and polarization of the exciton fine structure in single self-assembled InAs/GaAs quantum dots. Physical Review B, 2011, 83, .	1.1	28
52	Time-resolved ARPES Determination of a Quasi-Particle Band Gap and Hot Electron Dynamics in Monolayer MoS ₂ . Nano Letters, 2021, 21, 7363-7370.	4.5	28
53	Antimony Semimetal Contact with Enhanced Thermal Stability for High Performance 2D Electronics. , 2021, , .		28
54	Single photon emission from an InGaAs quantum dot precisely positioned on a nanoplane. Applied Physics Letters, 2007, 90, 073105.	1.5	27

#	Article	IF	CITATIONS
55	Low-Threshold Plasmonic Lasers on a Single-Crystalline Epitaxial Silver Platform at Telecom Wavelength. ACS Photonics, 2017, 4, 1431-1439.	3.2	27
56	Atomic-Layer Controlled Interfacial Band Engineering at Two-Dimensional Layered PtSe ₂ /Si Heterojunctions for Efficient Photoelectrochemical Hydrogen Production. ACS Nano, 2021, 15, 4627-4635.	7.3	27
57	Electroreflectance study on the polarization field in InGaN/AlInGaN multiple quantum wells. Applied Physics Letters, 2004, 84, 1114-1116.	1.5	26
58	Graphene-Au nanoparticle based vertical heterostructures: A novel route towards high- ZT Thermoelectric devices. Nano Energy, 2017, 38, 385-391.	8.2	26
59	Electroreflectance studies of InAs quantum dots with InxGa1â^'xAs capping layer grown by metalorganic chemical vapor deposition. Applied Physics Letters, 2005, 86, 131917.	1.5	23
60	Strong coupling of different cavity modes in photonic molecules formed by two adjacent microdisk microcavities. Optics Express, 2010, 18, 23948.	1.7	23
61	Time-resolved photoluminescence of isoelectronic traps in ZnSe1â^'xTex semiconductor alloys. Applied Physics Letters, 2008, 93, .	1.5	22
62	Designer germanium quantum dot phototransistor for near infrared optical detection and amplification. Nanotechnology, 2015, 26, 055203.	1.3	22
63	Monolayer MoS ₂ Enabled Single-Crystalline Growth of AlN on Si(100) Using Low-Temperature Helicon Sputtering. ACS Applied Nano Materials, 2019, 2, 1964-1969.	2.4	22
64	Ultralow Schottky Barriers in Hexagonal Boron Nitride-Encapsulated Monolayer WSe ₂ Tunnel Field-Effect Transistors. ACS Applied Materials & Interfaces, 2020, 12, 18667-18673.	4.0	22
65	Electron distribution and level occupation in an ensemble ofInxGa1â^'xAs/GaAsself-assembled quantum dots. Physical Review B, 2000, 62, 13040-13047.	1.1	21
66	Optical fine structures of highly quantized InGaAs/GaAs self-assembled quantum dots. Physical Review B, 2010, 81, .	1.1	21
67	Optical control of the exciton charge states of single quantum dots via impurity levels. Physical Review B, 2005, 72, .	1.1	20
68	Studies on the electronic and vibrational states of colloidal CdSe/ZnS quantum dots under high pressures. Nanotechnology, 2007, 18, 185402.	1.3	20
69	Epitaxial Growth of Optically Thick, Single Crystalline Silver Films for Plasmonics. ACS Applied Materials & Interfaces, 2019, 11, 3189-3195.	4.0	20
70	1.55μm emission from InAs quantum dots grown on GaAs. Applied Physics Letters, 2005, 87, 151903.	1.5	19
71	Carrier dynamics in isoelectronic ZnSe1â^'xOx semiconductors. Applied Physics Letters, 2010, 97, 041909.	1.5	19
72	Anomalous diamagnetic shift for negative trions in single semiconductor quantum dots. Physical Review B, 2010, 81, .	1.1	19

5

#	Article	IF	CITATIONS
73	Temperature-dependent optical and vibrational properties of PtSe2 thin films. Scientific Reports, 2020, 10, 19003.	1.6	19
74	Electron-filling modulation reflectance in charged self-assembledInxGa1â^'xAsquantum dots. Physical Review B, 1999, 60, R2189-R2192.	1.1	18
75	Impacts of ammonia background flows on structural and photoluminescence properties of InN dots grown on GaN by flow-rate modulation epitaxy. Applied Physics Letters, 2006, 89, 263117.	1.5	18
76	Effect of donor-acceptor concentration ratios on nonradiative energy transfer in closely packed CdTe quantum dots. Applied Physics Letters, 2009, 95, 133123.	1.5	17
77	Distance dependence of energy transfer from InGaN quantum wells to graphene oxide. Optics Letters, 2013, 38, 2897.	1.7	16
78	Optical properties associated with strain relaxations in thick InGaN epitaxial films. Optics Express, 2014, 22, A416.	1.7	16
79	Distributed Bragg Reflectors as Broadband and Large-Area Platforms for Light-Coupling Enhancement in 2D Transition-Metal Dichalcogenides. ACS Applied Materials & Interfaces, 2018, 10, 16874-16880.	4.0	16
80	Atomic-Step-Induced Screw-Dislocation-Driven Spiral Growth of SnS. Chemistry of Materials, 2021, 33, 186-194.	3.2	16
81	Excitation Density and Temperature Dependent Photoluminescence of InGaAs Self-Assembled Quantum Dots. Japanese Journal of Applied Physics, 1999, 38, 554-557.	0.8	15
82	Effects of growth temperature on InNâ^•GaN nanodots grown by metal organic chemical vapor deposition. Journal of Applied Physics, 2008, 103, 104306.	1.1	15
83	Stress tuning of strong and weak couplings between quantum dots and cavity modes in microdisk microcavities. Physical Review B, 2011, 84, .	1.1	15
84	Ultrafast Exciton Trapping and Exciton–Exciton Annihilation in Large-Area CVD-Grown Monolayer WS ₂ . Journal of Physical Chemistry C, 2021, 125, 23880-23888.	1.5	15
85	Nonresonant carrier transfer in single InGaAs/GaAs quantum dot molecules. Physical Review B, 2008, 77, .	1.1	14
86	Polymerâ€Free Patterning of Graphene at Subâ€10â€nm Scale by Lowâ€Energy Repetitive Electron Beam. Small, 2014, 10, 4778-4784.	5.2	14
87	A study of the Franz–Keldysh oscillations in electromodulation reflectance of Si-delta-doped GaAs by a fast Fourier transformation. Journal of Applied Physics, 1998, 83, 7873-7878.	1.1	13
88	Effect of focused ion beam deposition induced contamination on the transport properties of nano devices. Nanotechnology, 2015, 26, 055705.	1.3	13
89	Recombination dynamics and carrier lifetimes in highly mismatched ZnTeO alloys. Applied Physics Letters, 2013, 103, .	1.5	12
90	Atomic scale depletion region at one dimensional MoSe2-WSe2 heterointerface. Applied Physics Letters, 2018, 113, .	1.5	12

#	Article	IF	CITATIONS
91	Growth of low density InGaAs quantum dots for single photon sources by metal–organic chemical vapour deposition. Nanotechnology, 2006, 17, 512-515.	1.3	11
92	Growth of sparse arrays of narrow GaN nanorods hosting spectrally stable InGaN quantum disks. Optics Express, 2012, 20, 16166.	1.7	11
93	Suppressed piezoelectric polarization in single InGaN/GaN heterostructure nanowires. Physical Review B, 2013, 88, .	1.1	11
94	Effect of Electrode Shape on Impedance of Single HeLa Cell: A COMSOL Simulation. BioMed Research International, 2015, 2015, 1-9.	0.9	11
95	Optical properties of stacked Ge/Si quantum dots with different spacer thickness grown by chemical vapor deposition. Applied Surface Science, 2004, 224, 148-151.	3.1	10
96	Enhanced light emission from InAs quantum dots in single-defect photonic crystal microcavities at room temperature. Applied Physics Letters, 2005, 87, 071111.	1.5	10
97	Impacts of Coulomb Interactions on the Magnetic Responses of Excitonic Complexes in Single Semiconductor Nanostructures. Nanoscale Research Letters, 2010, 5, 680-685.	3.1	10
98	Growth of optical-quality, uniform In-rich InGaN films using two-heater metal-organic chemical vapor deposition. Journal of Crystal Growth, 2013, 383, 106-111.	0.7	10
99	Cross-plane thermoelectric figure of merit in graphene - C60 heterostructures at room temperature. FlatChem, 2019, 14, 100089.	2.8	10
100	Using Exciton/Trion Dynamics to Spatially Monitor the Catalytic Activities of MoS ₂ during the Hydrogen Evolution Reaction. ACS Nano, 2022, 16, 4298-4307.	7.3	10
101	Linear photon up-conversion of 450 meV in InGaN/GaN multiple quantum wells via Mn-doped GaN intermediate band photodetection. Optics Express, 2011, 19, A1211.	1.7	9
102	Efficient energy transfer from InGaN quantum wells to Ag nanoparticles. Physical Chemistry Chemical Physics, 2013, 15, 3618.	1.3	9
103	Memory device application of wide-channel in-plane gate transistors with type-II GaAsSb-capped InAs quantum dots. Applied Physics Letters, 2013, 103, 143502.	1.5	9
104	Hybrid Composites of Quantum Dots, Monolayer WSe ₂ , and Ag Nanodisks for White Light-Emitting Diodes. ACS Applied Nano Materials, 2020, 3, 6855-6862.	2.4	9
105	Strain-Directed Layer-By-Layer Epitaxy Toward van der Waals Homo- and Heterostructures. , 2021, 3, 442-453.		9
106	Roomâ€Temperature Ferromagnetism of Single‣ayer MoS ₂ Induced by Antiferromagnetic Proximity of Yttrium Iron Garnet. Advanced Quantum Technologies, 2021, 4, 2000104.	1.8	9
107	Ultrafast laser ablation, intrinsic threshold, and nanopatterning of monolayer molybdenum disulfide. Scientific Reports, 2022, 12, 6910.	1.6	9
108	Low temperature deposition of high quality single crystalline AlN thin films on sapphire using highly oriented monolayer MoS2 as a buffer layer. Journal of Crystal Growth, 2020, 544, 125726.	0.7	8

#	Article	IF	CITATIONS
109	Enhancing luminescence efficiency of InAs quantum dots at 1.5î¼m using a carrier blocking layer. Applied Physics Letters, 2006, 89, 053110.	1.5	7
110	Structural and optical properties of In-rich InGaN nanodots grown by metallo-organic chemical vapor deposition. Nanotechnology, 2007, 18, 405305.	1.3	7
111	Pressure-induced metallization and resonant Raman scattering in Zn1â^'xMnxTe. Journal of Applied Physics, 2008, 104, 013503.	1.1	7
112	Recombination lifetimes in InN films studied by time-resolved excitation-correlation spectroscopy. Physical Review B, 2009, 80, .	1.1	7
113	Effects of oxygen bonding on defective semiconducting and metallic single-walled carbon nanotube bundles. Carbon, 2012, 50, 4619-4627.	5.4	7
114	Band alignment tuning of InAs quantum dots with a thin AlGaAsSb capping layer. Applied Physics Letters, 2013, 102, .	1.5	7
115	Efficient modulation of subwavelength focusing via meta-aperture-based plasmonic lens for multifunction applications. Scientific Reports, 2018, 8, 13648.	1.6	7
116	Two-dimensional solid-phase crystallization toward centimeter-scale monocrystalline layered MoTe ₂ <i>via</i> two-step annealing. Journal of Materials Chemistry C, 2021, 9, 15566-15576.	2.7	7
117	A Carrier Escape Study from InAs Self-Assembled Quantum Dots by Photocurrent Measurement. Physica Status Solidi (B): Basic Research, 2001, 224, 85-88.	0.7	6
118	Three-Dimensional Resolvable Plasmonic Concentric Compound Lens: Approaching the Axial Resolution from Microscale to Nanoscale. ACS Photonics, 2018, 5, 834-843.	3.2	6
119	Nitride-stressor and quantum-size engineering in Ge quantum-dot photoluminescence wavelength and exciton lifetime. Nano Futures, 2020, 4, 015001.	1.0	6
120	Fast Fourier transformation of piezoreflectance in δ-doped GaAs. Journal of Applied Physics, 1998, 84, 1074-1080.	1.1	5
121	Room temperature 1.3 and 1.5 μm electroluminescence from Si/Ge quantum dots (QDs)/Si multi-layers. Applied Surface Science, 2004, 224, 165-169.	3.1	5
122	Raman scattering of longitudinal-optical-phonon-plasmon coupling in Cl-doped ZnSe under high pressure. Journal of Applied Physics, 2007, 102, .	1.1	5
123	Timeâ€resolved photoluminescence of typeâ€l InAs/GaAs quantum dots covered by a thin GaAs _{1–x} Sb _x layer. Physica Status Solidi C: Current Topics in Solid State Physics, 2009, 6, 1449-1452.	0.8	5
124	Growth and optical properties of high-density InN nanodots. Journal of Crystal Growth, 2010, 312, 3209-3213.	0.7	5
125	Optical properties of Mn in regrown GaN-based epitaxial layers. Optical Materials Express, 2012, 2, 469.	1.6	5
126	In-Plane Gate Transistors for Photodetector Applications. IEEE Electron Device Letters, 2013, 34, 780-782.	2.2	5

#	Article	IF	CITATIONS
127	Stacking fault induced tunnel barrier in platelet graphite nanofiber. Applied Physics Letters, 2014, 105, 103505.	1.5	5
128	Influences of Contact Metals on the Performances of MoS ₂ Devices under Strains. Journal of Physical Chemistry C, 2019, 123, 30696-30703.	1.5	5
129	Carrier gas effects on the SiGe quantum dots formation. Applied Surface Science, 2008, 254, 6257-6260.	3.1	4
130	The structural and optical properties of InN nanodots grown with various V/III ratios by metal–organic chemical vapor deposition. Nanotechnology, 2009, 20, 295702.	1.3	4
131	Size-dependent strain relaxation in InN islands grown on GaN by metalorganic chemical vapor deposition. Applied Physics Letters, 2009, 94, 063102.	1.5	4
132	DC Characteristics of InAlAs/InGaAsSb/InGaAs Double Heterojunction Bipolar Transistors. IEEE Transactions on Electron Devices, 2010, 57, 3327-3332.	1.6	4
133	Tailoring of the Wave Function Overlaps and the Carrier Lifetimes in InAs/GaAs1â°'xSbx Type-II Quantum Dots. Physica E: Low-Dimensional Systems and Nanostructures, 2010, 42, 2524-2528.	1.3	4
134	Temperature-dependent decay dynamics in highly mismatched ZnSe1â^' <i>x</i> Te <i>x</i> alloy. Applied Physics Letters, 2012, 100, .	1.5	4
135	Boost Lasing Performances of 2D Semiconductor in a Hybrid Tungsten Diselenide Monolayer/Cadmium Selenide Quantum Dots Microcavity Laser. Advanced Optical Materials, 2022, 10, .	3.6	4
136	Effects of Electric Field and Coulomb Interaction on the Interband Transitions of InAs Self-Assembled Quantum Dots: A Study by Modulation Reflectance Spectroscopy. Physica Status Solidi (B): Basic Research, 2001, 224, 89-92.	0.7	3
137	Optical emission from individual InGaAs quantum dots in single-defect photonic crystal nanocavity. Journal of Applied Physics, 2005, 98, 034306.	1.1	3
138	Origins of nonzero multiple photon emission probability from single quantum dots embedded in photonic crystal nanocavities. Applied Physics Letters, 2009, 94, 163111.	1.5	3
139	Optical Properties of Uncapped InN Nanodots Grown at Various Temperatures. Japanese Journal of Applied Physics, 2009, 48, 031001.	0.8	3
140	Cathodoluminescence studies of GaAs nano-wires grown on shallow-trench-patterned Si. Nanotechnology, 2010, 21, 465701.	1.3	3
141	Energy transfer from InGaN quantum wells to Au nanoclusters via optical waveguiding. Optics Express, 2011, 19, A194.	1.7	3
142	Determination ofs-dexchange coupling in GaMnN by time-resolved Kerr rotation spectroscopy. Physical Review B, 2014, 90, .	1.1	3
143	Photoluminescence Enhancement in WS ₂ Nanosheets Passivated with Oxygen Ions: Implications for Selective Area Doping. ACS Applied Nano Materials, 2021, 4, 11693-11699.	2.4	3
144	Effect of ZnSe partial capping on the ripening dynamics of CdSe quantum dots. Applied Physics Letters, 2007, 90, 083116.	1.5	2

#	Article	IF	CITATIONS
145	Structural and optical properties of indium-rich InGaN islands. Physica Status Solidi C: Current Topics in Solid State Physics, 2008, 5, 1702-1705.	0.8	2
146	Structural and optical properties of InN/GaN nanodots grown by metalorganic chemical vapor deposition. Physica Status Solidi C: Current Topics in Solid State Physics, 2008, 5, 3014-3016.	0.8	2
147	Electron–hole symmetry breakings in optical fine structures of single self-assembled quantum dots. Physica E: Low-Dimensional Systems and Nanostructures, 2010, 42, 1155-1158.	1.3	2
148	Optical characterization of isoelectronic ZnSe1â^'O semiconductors. Journal of Crystal Growth, 2011, 323, 122-126.	0.7	2
149	Analysis of electrode shape effect on single HeLa cell impedance using COMSOL simulation. , 2013, , .		2
150	Optical detection of anisotropic <i>g</i> -factor and nuclear spin polarization in a single CdTe quantum well. Japanese Journal of Applied Physics, 2015, 54, 033003.	0.8	2
151	Design of multifold Ge/Si/Ge composite quantum-dot heterostructures for visible to near-infrared photodetection. Optics Letters, 2015, 40, 2401.	1.7	2
152	Synthesis of SiV-diamond particulates via the microwave plasma chemical deposition of ultrananocrystalline diamond on soda-lime glass fibers. Materials Research Express, 2016, 3, 106205.	0.8	2
153	Fabrication of Large-Scale High-Mobility Flexible Transparent Zinc Oxide Single Crystal Wafers. ACS Applied Materials & Interfaces, 2021, 13, 18991-18998.	4.0	2
154	Momentum-Resolved Electronic Structures of a Monolayer-MoS2/Multilayer-MoSe2 Heterostructure. Journal of Physical Chemistry C, 2021, 125, 16591-16597.	1.5	2
155	Ultrafast multi-shot ablation and defect generation in monolayer transition metal dichalcogenides. AIP Advances, 2022, 12, 015217.	0.6	2
156	Scanning electron filling modulation reflectance of charged InGaAs self-assembled quantum dot. Journal of Applied Physics, 2002, 91, 4399-4402.	1.1	1
157	Exciton fine structures and energy transfer in single InGaAs quantumâ€dot molecules. Physica Status Solidi C: Current Topics in Solid State Physics, 2009, 6, 860-863.	0.8	1
158	Magneto-optical properties of ZnMnTe/ZnSe quantum dots. Journal of Crystal Growth, 2011, 323, 380-382.	0.7	1
159	All-color plasmonic nanolasers with ultralow thresholds. , 2013, , .		1
160	Grain size effect of monolayer MoS2 transistors characterized by second harmonic generation mapping. , 2015, , .		1
161	Original method of GaN and InGaN quantum dots formation on (0001)AlN surface by ammonia molecular beam epitaxy. Journal of Physics: Conference Series, 2017, 864, 012007.	0.3	1
162	2D Materials: Metalâ€Guided Selective Growth of 2D Materials: Demonstration of a Bottomâ€Up CMOS Inverter (Adv. Mater. 18/2019). Advanced Materials, 2019, 31, 1970132.	11.1	1

#	Article	IF	CITATIONS
163	In Situ Atomic‣cale Observation of Monolayer MoS ₂ Devices under Highâ€Voltage Biasing via Transmission Electron Microscopy (Small 7/2022). Small, 2022, 18, .	5.2	1
164	Strain-induced material intermixing in multiple-stacked Ge/Si quantum dots grown by chemical vapor deposition. , 0, , .		0
165	Conductance mapping for the electron and hole energy levels in InAs/GaAs self-assembled quantum dots. , 0, , .		0
166	Room-temperature electroluminescence at 1.3 and 1.5 \hat{l} 4 m from Ge/Si quantum-dot light-emitting diode. , 0, , .		0
167	Single-photon emissions from individual InGaAs quantum dots in photonic crystal microcavity. , 2005, , .		0
168	Single photon sources based on single InGaAs quantum dots. , 2005, , .		0
169	Collective And Individual Emissions For InGaAs Quantum Dots In Photonic Crystal Nanocavity. AIP Conference Proceedings, 2007, , .	0.3	0
170	Optical Properties Of Exciton Charge States In InGaAs Quantum Dots Grown By Metalorganic Chemical Vapor Deposition. AIP Conference Proceedings, 2007, , .	0.3	0
171	Direct near-field mapping of photoelectric response induced by localized surface plasmon of silver nano-islands on a silicon solar cell. , 2012, , .		Ο
172	Enhanced optical absorption induced by localized surface plasmon of gold nanospheres in a silicon solar cell. , 2013, , .		0
173	Fast visible-light phototransistor using CVD-synthesized large-area bilayer WSe <inf>2</inf> . , 2014, , .		0
174	Waveguide based energy transfer with gold nanoclusters for detection of hydrogen peroxide. RSC Advances, 2014, 4, 30392-30397.	1.7	0
175	Plasmonic whispering-gallery modes in a semiconductor-insulator-metal hybrid structure. , 2015, , .		0
176	2D Layered Semiconductors beyond MoS2. , 2019, , .		0
177	Low-density quantum dots embedded in photonic-crystal nanocavities for single-photon generations. AIP Conference Proceedings, 2007, , .	0.3	0
178	Nanolasers Employing Epitaxial Plasmonic Layers. , 2013, , .		0
179	Photoluminescence Enhancement in Defect Monolayer MoSe2 by Hydrohalic Acid Treatment. , 2016, , .		0
180	Femtosecond-Laser Ablation of Monolayer Tungsten Diselenide (WSe2) on Sapphire. , 2018, , .		0

#	Article	IF	CITATIONS
181	Femtosecond-laser ablation of monolayer molybdenum disulfide (MoS2) on sapphire. , 2019, , .		Ο
182	Investigation of the spectral characteristics of silicon-vacancy centers in ultrananocrystalline diamond nanostructures and single crystalline diamond. Journal of Applied Physics, 2020, 127, 035302.	1.1	0